Available online at www.sciencedirect.com
ScienceDirect
Journal of Organometallic Chemistry 692 (2007) 5541–5548
Journal of Organometallic Chemistry
www.elsevier.com/locate/jorganchem

# Structures and electronic states of paramagnetic species in Al–NTCDA co-deposit films

Hiroto Tachikawa [a,*], Hiroshi Kawabata [b]

[a] Division of Materials Chemistry, Graduate School of Engineering, Hokkaido University, Sapporo 060-8628, Japan
[b] Department of Electronic Science and Engineering, Kyoto University, Nishikyo-ku, Kyoto 615-8510, Japan

Received 27 June 2007; received in revised form 20 August 2007; accepted 23 August 2007
Available online 14 September 2007

**Abstract**

Structures and electronic states of paramagnetic species in co-deposit film composed of 1,4,5,8-naphthalene-tetracarboxylic-dianhydride (NTCDA) and aluminum (Al) have been investigated by means of hybrid density functional theory (DFT) calculations to determine the species in detail. Al–NTCDA 1:1 complex, 1:3 $Al_3$–NTCDA complex and an Al metal bridged dimer Al–$(NTCDA)_2$ were examined as paramagnetic species of Al–NTCDA complexes. The simulated electron paramagnetic resonance (EPR) spectra of the 1:3 complex and the dimer were in reasonable agreement with experiment reported previously by Tachikawa et al. [Tachikawa et al., J. Phys. Chem. B 109 (2005) 3139]. It was found that the contribution from the 1:1 complex to the EPR spectra was very small. From the comparison with theoretical and experimental UV and EPR spectra, it was found that several paramagnetic and diamagnetic species exist in the co-deposit film of Al/NTCDA. The structures and electronic states were discussed on the basis of theoretical results.


*Keywords:* Organic–inorganic hybrid complex; NTCDA; Al–NTCDA; EPR; Paramagnetic species; DFT calculation

## 1. Introduction

Thin films of molecular organic semiconductors have been attractive much interest for use as electronic and optoelectronic applications. In particular, an organic–inorganic hybrid complex is one of the high performance molecular devices utilized for field effect transistor (FET) in flexible displays [1,2] and in smart tags [3,4].

1,4,5,8-Naphthalene tetracarboxylic dianhydride (NTCDA) is one of the high-performance molecular devices utilized for photo-current multiplications and organic semiconductors. NTCDA has four C=O carbonyl groups in its molecule. By the interaction with metal atoms, the electron conductivity increases up to the order of $10^{-2}$ S/cm. For example, the electron conductivity of free NTCDA ($\sigma = 10^{-8}$ S/cm) is drastically changed to $\sigma = 5.0 \times 10^{-5}$ S/cm (Al), $\sigma = 2.3 \times 10^{-5}$ S/cm (Mg) and $\sigma = 1.3 \times 10^{-2}$ S/cm (In) interacting with aluminum, magnesium and indium atoms, respectively. These results indicate that the electron conductivity increases about 3–5 orders of magnitude by the co-deposition of NTCDA and metal atoms (M) [5,6].

In previous papers [7–9], we investigated a hybrid complex composed of NTCDA and 3,4,9,10-perylene-tetracarboxylicacid-dianhydride (PTCDA) with metals using FT-IR, ESR and absorption spectroscopic techniques and density functional theory (DFT) calculation. The mechanism of electron conductivity in M-NTCDA and M-PTCDA was proposed on the basis of experimental and theoretical results. As a model of Al–NTCDA interaction system, we considered $Al_n$–NTCDA complex ($n = 1$–4) in previous paper. The absorption spectra of these complexes in UV and visible regions are in good agreement with the experiment. However, ESR spectrum of Al–NTCDA suggested that the paramagnetic species are contaminated into the Al–NTCDA co-deposit film.

In the present study, to elucidate the structures and electronic states of Al–NTCDA system in more detail, DFT

* Corresponding author. Fax: +81 11706 7897.
*E-mail address:* hiroto@eng.hokudai.ac.jp (H. Tachikawa).

0022-328X/$ - see front matter © 2007 Elsevier B.V. All rights reserved.
doi:10.1016/j.jorganchem.2007.08.041

calculations have been applied to the Al–NTCDA system. We focus our attention mainly on paramagnetic species existing in the Al–NTCDA co-deposit film which is not determined experimentally. As a model system, the metal (Al) bridged-NTCDA dimer, where the Al atom interacts with two NTCDA molecule, is examined as well as $(Al)_n$–NTCDA ($n = 1$ and 3).

In previous works [7–9], we investigated the structures and electronic states of PTCDA [8], which is the similar molecular semiconductor to NTCDA, and its complexes with the In atom. We suggested that the In atom can bind strongly to the carbonyl group of PTCDA. Also, we investigated mechanism of electron and hole conductivities in molecular devices, such as poly-vinylbiphenyl (PVB) [10] and polysilanes [11], by means of ab initio DFT and ab initio molecular dynamics (MD) methods [12]. In the present work, we extend previous techniques to the Al–NTCDA system.

## 2. Method of calculation

All hybrid DFT calculations were carried out using GAUSSIAN 03 program package [13]. As paramagnetic species, Al–NTCDA (denoted by 1:1 complex), $Al_3$–NTCDA (3:1 complex), and the aluminum Al bridged-NTCDA expressed by Al–$(NTCDA)_2$ (denoted by bridged-dimer) were considered in the present study. The geometries of these species were fully optimized at the B3LYP/6-31G(d), B3LYP/6-311G(d,p) and B3LYP/6-311+G(d,p) levels of theory. Since those levels of theory gave the similar optimized structures and electronic states of the present system, we discuss the structure and electronic states using the most sophisticated level, i.e, B3LYP/6-311+G(d,p), in the present study throughout. Using the optimized geometries, the excitation energies were calculated by means of time-dependent (TD) DFT calculation at the B3LYP/6-311+G(d,p) level. Nine states were solved in all systems. The electronic states of all molecules were obtained by natural population analysis (NPA) method. These methods and the levels of theory give a reasonable feature for metal and organic systems.

## 3. Results

### 3.1. Structures of Al–NTCDA and Al$(NTCDA)_2$

The geometries of free NTCDA molecule, Al–NTCDA, $Al_3$–NTCDA and $Al(NTCDA)_2$ are optimized and the structures are illustrated in Fig. 1. The optimized parameters are given in Table 1. In free NTCDA, the bond lengths of the C=O carbonyl, the carbon–carbon single bond, and the C–O single bond in naphthalene part are calculated to be $r(C_1{=}O_1) = 1.196$, $r(C_1{-}C_2) = 1.483$, and $r(C_1{-}O_2) = 1.388$ Å, respectively.

In Al–NTCDA, aluminum atom is bound to the oxygen atom of the C=O carbonyl group of NTCDA. The distance of Al atom from the oxygen atom is $r$(Al–O) = 1.796 Å and the angle of C–O–Al is 151.1°. By the interaction with the Al atom, the bond length of the C=O carbonyl is elongated from 1.196 to 1.301 Å and that of $C_1$–$C_2$ bond is shortened from 1.483 to 1.393 Å. The C–O single bond $r(C_1{-}O_2)$ is slightly changed from 1.388 to 1.349 Å. In the 1:3 complex, the distances of Al atom from the oxygen atoms are $r$(Al–O) = 1.756, 1.773, and 1.757 Å, which are close to that of the 1:1 complex.

In the metal bridged-NTCDA dimer $Al(NTCDA)_2$, the Al atom is located in the central position between the oxygen atoms of two NTCDA molecules. The distance of $r$(Al–O) is calculated to be 2.261 Å, and the angle of O–Al–O is 139.4°, indicating that the Al–O distances are largely elongated by the dimer formation. The bond distance of the C=O carbonyl group of NTCDA is slightly shortened from 1.483 to 1.442 Å by the dimer formation. This distance is significantly longer than that of 1:1 Al–NTCDA complex (1.301 Å).

### 3.2. Binding energies of Al atom to NTCDA

The binding energies of Al atom to NTCDA are given in Table 2. The most sophisticated method, the B3LYP/6-311+G(d,p) level, shows the binding energies of Al atom to free NTCDA is 55.5 kcal/mol. In the bridged dimer system, the binding energy is 45.5 kcal/mol and the binding energy per one Al–O bond is 22.8 kcal/mol which is large enough to form the bridged dimmer. The binding energies for $n = 1$ and 3 are calculated to be 55.5 (27.8) kcal/mol and 161.2 (53.7) kcal/mol, respectively, where the values in parenthesis indicate the binding energy per one Al–O bond.

The atomic charges obtained by the natural population analysis (NPA) are given in Table 3. The charges of the C=O carbonyl of free NTCDA are calculated to be +0.79 ($C_1$) and −0.51 ($O_1$). By the interacting with an aluminum atom (formation of the 1:1 Al–NTCDA complex), the charges are changed to 0.50 ($C_1$) and −0.47 ($O_1$), while the charge of Al is +0.44. This value indicates that 60% of electron of Al is transferred to the NTCDA molecule in the 1:1 complex. The average charge of Al atom in the 1:3 complex is 0.42 which is close to that of the 1:1 complex and dimer. In the case of the bridged dimer, the natural charge of the Al atom is calculated to be +0.46, indicating that the charge on NTCDA becomes half of the 1:1 complex after the formation of the neutral bridged dimer.

### 3.3. Excitation energies of Al–NTCDA

The excited states correlate strongly to the electron conductivity organic semi-conductor. Hence, in the present study, the electronic structures for the excited states are determined by means of time-dependent (TD)-DFT method. The results are given in Table 4 and Fig. 2. First, the excitation energies of free NTCDA are calculated. The first excited state corresponds to the $^1B_{1u}$ state, and the excitation energy is calculated to be 3.40 eV. The electronic

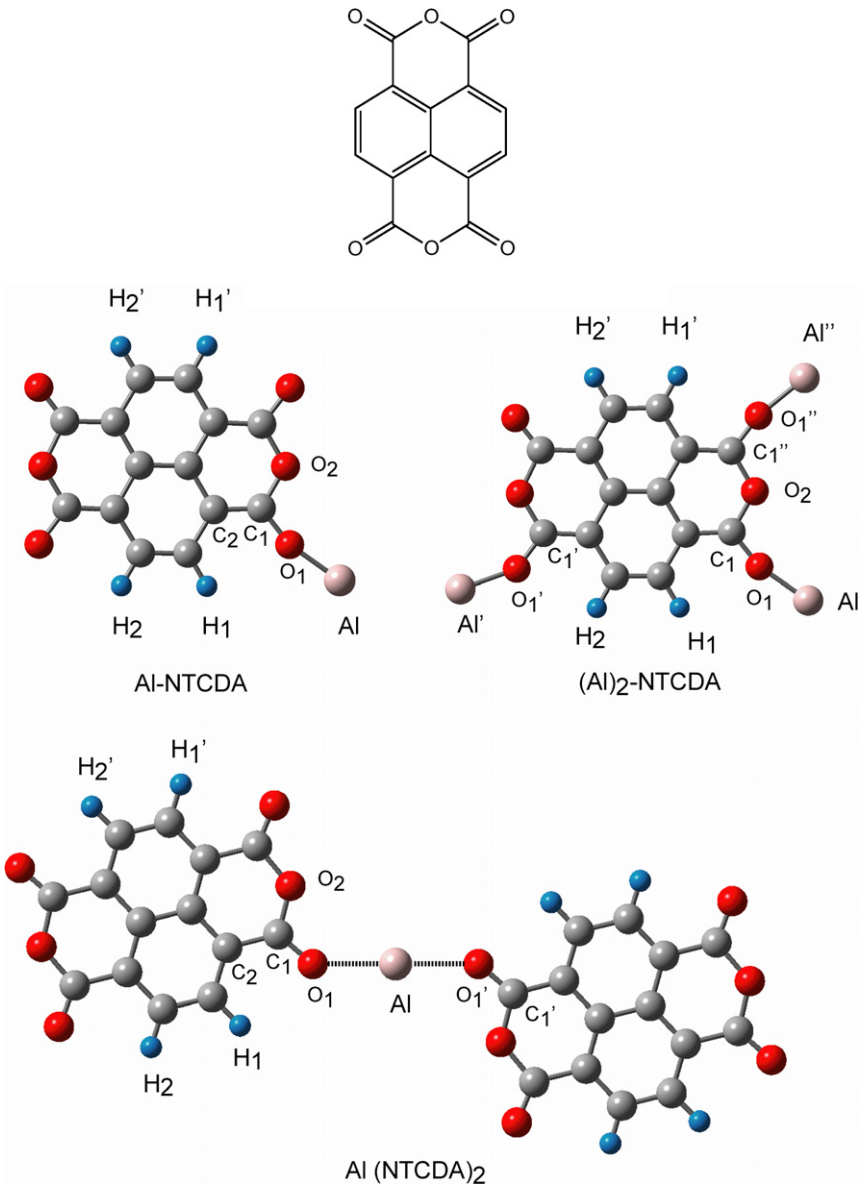


Fig. 1. Optimized structures of Al–NTCDA (1:1 complex: $n = 1$), $Al_3$–NTCDA (3:1 complex: $n = 3$), and Al–$(NTCDA)_2$ (aluminum bridged NTCDA dimer) calculated at the B3LYP/6-311+G(d,p) level.

Table 1
Optimized parameters of NTCDA, Al–NTCDA (1:1 complex), $Al_3$–NTCDA (3:1 complex), and Al–$(NTCDA)_2$ (aluminum bridged NTCDA dimer) calculated at the B3LYP/6-311+G(d,p) level

| Parameter | System | | | |
|---|---|---|---|---|
| | NTCDA | Al–NTCDA | $Al_3$–NTCDA | Al–$(NTCDA)_2$ |
| $r(C_1{=}O_1)$ | 1.1956 | 1.3006 | 1.3136 | 1.2393 |
| $r(C_1{-}O_2)$ | 1.3879 | 1.3490 | 1.3755 | 1.3583 |
| $r(C_1{-}C_2)$ | 1.4828 | 1.3930 | 1.3655 | 1.4417 |
| $r(Al{-}O_1)$ | | 1.7956 | 1.7558 | 2.2607 |
| $r(Al'{-}O_1')$ | | | 1.7732 | 2.2607 |
| $r(Al''{-}O_1')$ | | | 1.7567 | |
| $\angle C_1$-$O_1$-Al | | 151.1 | 163.2 | 139.4 |
| $\angle C_1'{-}O_1'{-}Al'$ | | | 146.4 | |
| $\angle C_1'{-}O_1'{-}Al''$ | | | 167.0 | |

Bond lengths and angles are in Å and in °, respectively.

transition from the ground to first excited states, $^1Ag \rightarrow {}^1B_{1u}$, is "symmetry allowed" with a large oscillator strength ($f = 0.258$), which is large enough to observe experimentally as an absorption band. It should be noted that the first excitation energy of NTCDA is observed experimentally to be 3.20 eV, which is in reasonable agreement with the present TD-DFT calculation (3.40 eV). The agreement implies that the TD-DFT calculation at the B3LYP/6-311+G(d,p) level would give a reasonable feature for the excitation energy and electronic structure for the excited states of the NTCDA system.

For the 1:1 Al–NTCDA complex, the excitation energies with non zero intensities are calculated to be 1.71 eV ($f = 0.060$), 2.34 eV ($f = 0.003$) and 2.54 eV ($f = 0.164$). This result implies that the excitation energies of NTCDA are strongly affected by the complex formation with the Al

Table 2
Binding energies of Al atom to NTCDA (in kcal/mol)

| System | Symmetry | B3LYP/6-31G(d) | B3LYP/6-311G(d,p) | B3LYP/6-311+G(d,p) |
|---|---|---|---|---|
| Al–NTCDA | $C_1$ | 54.3 | 54.7 | 55.5 (27.7) |
| $Al_3$–NTCDA | $C_s$ | 158.7 (52.9) | 159.5 (53.2) | 161.18 (53.7) |
| Al–$(NTCDA)_2$ | $C_{2h}$ | 44.8 (22.4) | 45.1 (22.6) | 45.53 (22.8) |

Binding energies per one Al–O bond are given in parenthesis (in kcal/mol).

Table 3
Natural charges on atoms of NTCDA and Al–NTCDA systems calculated by means of natural population analysis (NPA) at the B3LYP/6-311+G(d,p) level

| Atom | NTCDA | Al–NTCDA | $Al_3$–NTCDA | Al–$(NTCDA)_2$ |
|---|---|---|---|---|
| $C_1$ | 0.794 | 0.500 | 0.371 | 0.449 |
| $O_1$ | −0.511 | −0.471 | −0.509 | −0.364 |
| $C_2$ | −0.170 | −0.117 | −0.100 | −0.077 |
| $O_2$ | −0.542 | −0.262 | −0.214 | −0.277 |
| ⟨Al⟩[a] | | 0.441 | 0.422 | 0.455 |

[a] Average of charges of three aluminum atoms (Al = 0.419, Al′ = 0.418, Al″ = 0.430).

Table 4
Excitation energies (in eV) of NTCDA, Al–NTCDA, $Al_3$–NTCDA, and Al–$(NTCDA)_2$

| State | NTCDA | Al–NTCDA | $Al_3$–NTCDA | Al–$(NTCDA)_2$ |
|---|---|---|---|---|
| 1st | 3.40 (0.2576) | 1.71 (0.0599) | 1.16 (0.0179) | 0.26 (0.0942) |
| 2nd | 3.42 (0.0000) | 2.34 (0.0026) | 1.44 (0.0000) | 1.42 (0.0000) |
| 3rd | 3.58 (0.0002) | 2.44 (0.0000) | 1.58 (0.1246) | 1.56 (0.0395) |
| 4th | 3.78 (0.0671) | 2.54 (0.1643) | 1.62 (0.0000) | 2.00 (0.0000) |
| 5th | 3.95 (0.0000) | 2.80 (0.0061) | 1.72 (0.0864) | 2.00 (0.0000) |
| 6th | 4.20 (0.0000) | 2.88 (0.0000) | 1.77 (0.0309) | 2.09 (0.0078) |
| 7th | 4.38 (0.0000) | 2.98 (0.0004) | 1.86 (0.0000) | 2.09 (0.0000) |
| 8th | 4.90 (0.0000) | 3.05 (0.0595) | 1.99 (0.0254) | 2.09 (0.0000) |
| 9th | 4.92 (0.0000) | 3.11 (0.0000) | 2.17 (0.0009) | 2.43 (0.0014) |

Oscillator strengths are given in parenthesis. The values are calculated at the B3LYP/6-311+G(d,p) level.

atom. Also, it is found that the band gap becomes significantly lower in the complex formation (3.40 → 1.71 eV). By the formation of the 3:1 complex, several low excitation bands are appeared in the energy range 1.16–2.17 eV.

In the case of Al-bridged NTCDA dimmer, the first excitation energy with non-zero oscillator strength in the visible region is appeared at 1.56 eV ($f = 0.040$), which is 0.15 eV red-shifted from that of A1–NTCDA. Also, it is found that a low-lying energy level is appeared at 0.26 eV by the dimer formation. This level can be assigned to be a charge resonance band between two NTCDA molecules. Since this transition has a finite oscillator strength ($f = 0.094$), thermal excitation to the level would be contributed strongly the electron conductivity along the molecular plane.

In order to assign the absorption band appearing at low energy region in the Al bridged NTCDA dimer, the weight of the reference functions is analyzed. The main configuration for the excited state at visible region (1.56 eV) is consisted of a transition form SOMO(143) → LUMO+2 (146) with a weight of 0.984, where SOMO and LUMO mean singly occupied molecular orbital and lowest unoccupied

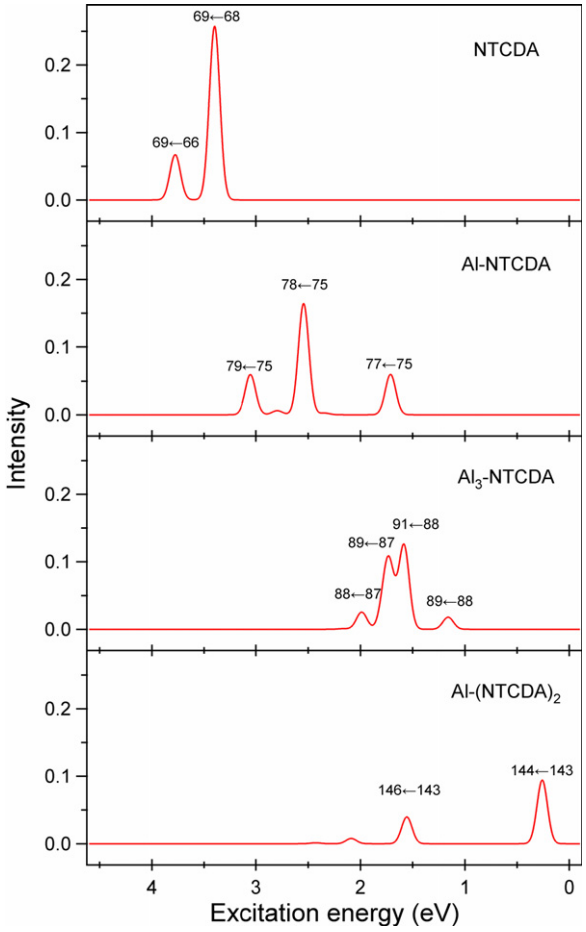


Fig. 2. Simulated absorption spectra of Al–NTCDA, $Al_3$–NTCDA, and Al–$(NTCDA)_2$ calculated at the B3LYP/6-311+G(d,p) level. Gaussian function is assumed for each peak and half-value width is fixed to 0.05 eV. Number indicates molecular orbital number of main configuration contributes the excitation.

molecular orbital, respectively. Here, number in parenthesis means the orbital number contributing to the main configuration. The SOMO (143), LUMO (144), and LUMO+2 (146) of the metal bridged NTCDA dimer are illustrated by iso-surface in Fig. 3. The SOMO is mainly composed of π-orbitals delocalized over two NTCDA molecules and π-orbital of the Al atom. The 3p orbital of Al contributes also the component of SOMO. In the case of LUMO, the orbital phase of two NTCDA molecules are reversed each other and a node of orbital phase is just located in the position of Al. The excitation band at visible region is assigned to a $\pi$–$\pi^*$ transition including a slight electron transfer from the metal to NTCDA.

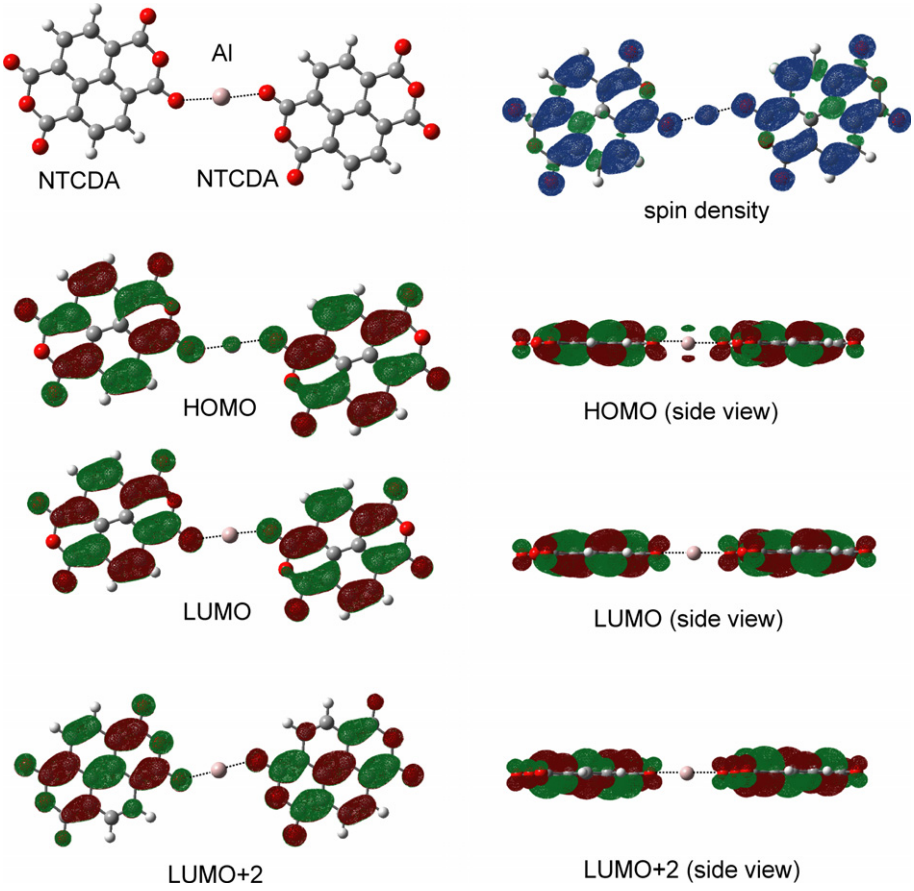


Fig. 3. Spin density and molecular orbitals (HOMO, LUMO and LUMO+2) of Al–$(NTCDA)_2$ (aluminum bridged NTCDA dimer) calculated at the B3LYP/6-311+G(d,p) level.

### 3.4. Simulated ESR spectra of the aluminum bridged-NTCDA dimer

NTCDA molecule has four hydrogen atoms in the backbone. Hence, ESR spectrum would be observed if NTCDA is a doublet state. In our previous paper [7], we observed experimentally that co-deposit film of Al/NTCDA system shows a single line EPR spectrum without hyperfine structure. Hence, theoretical EPR simulation would give important information on the paramagnetic species in the co-deposit film. The hydrogen hyperfine coupling constant (H-hfcc's) are given in Table 5. The hfcc's of Al–NTCDA are calculated to be −5.64 G ($H_1$), 1.35 G ($H_2$), −3.01 G ($H_1'$), 0.67 G ($H_2'$). After the formation of the bridged dimer, these values are changed to −2.05 G ($H_1$), 0.0 G ($H_2$), −1.48 G ($H_1'$), −0.09 G ($H_2'$), indicating that the H-hfcc's of Al–NTCDA becomes significantly lower by the formation of the bridged dimer. The hfcc's of the 3:1 complex are calculated to be 0.0 G ($H_1$), 0.0 G ($H_2$), −2.92 G ($H_1'$), 1.47 G ($H_2'$), which is close to those of the bridged dimer.

The spin densities on atoms are given in Table 6. The spin densities on Al atoms are similar each other (0.03). The $g$ values for three species are calculated to be 2.0030, which is larger than that of free electron ($g_e = 2.0023$), indicating that all species can be candidate of the paramagnetic species.

Using these parameters, ESR spectra are simulated as a function of half width (denoted by $d$) and the results are given in Fig. 4. If $d$ is assumed to 0.05 G, the spectra of

Table 5
Hydrogen-hyperfine coupling constants (hfcc's in G) of NTCDA, $Al_3$–NTCDA, and Al–NTCDA systems calculated at the B3LYP/6-311+G(d,p) level

| Atom | Al–NTCDA | $Al_3$–NTCDA | Al–$(NTCDA)_2$ |
|---|---|---|---|
| $H_1$ | −5.642 | −0.013 | −2.046 |
| $H_2$ | 1.348 | 0.002 | 0.002 |
| $H_3$ | −3.006 | −2.923 | −1.477 |
| $H_4$ | 0.666 | 1.473 | −0.094 |

Table 6
Atomic spin densities of NTCDA, $Al_3$–NTCDA, and Al–NTCDA systems calculated at the B3LYP/6-311+G(d,p) level

| Atom | Al–NTCDA | $Al_3$–NTCDA | Al–$(NTCDA)_2$ |
|---|---|---|---|
| $C_1$ | 0.253 | 0.073 | 0.061 |
| $O_1$ | 0.037 | 0.000 | 0.030 |
| $C_2$ | −0.056 | −0.009 | 0.0097 |
| $O_2$ | 0.006 | 0.085 | −0.006 |
| ⟨Al⟩[a] | 0.026 | 0.032 | 0.028 |

[a] Average of atomic spin densities of three aluminum atoms (Al = 0.021, Al′ = 0.007, Al″ = 0.070).

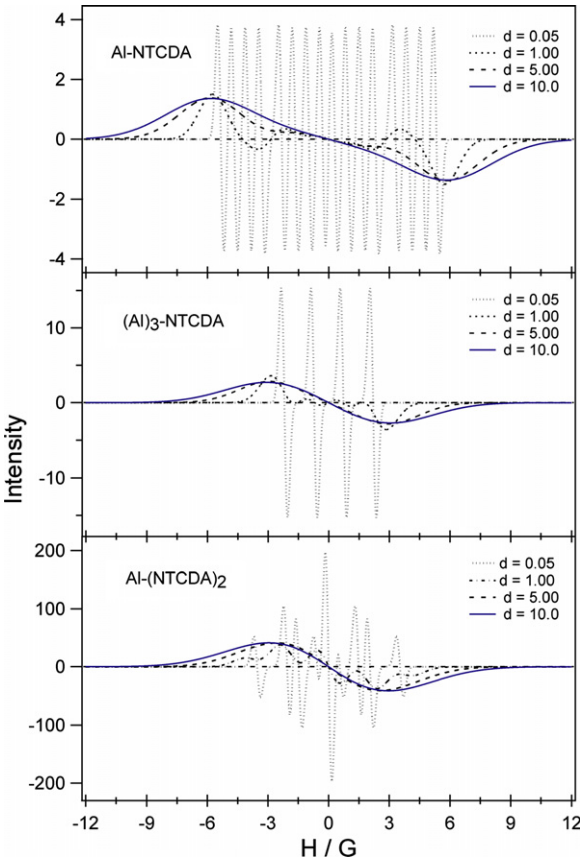


Fig. 4. Simulated ESR spectra of Al–NTCDA, $Al_3$–NTCDA, and Al–$(NTCDA)_2$ calculated at the B3LYP/6-311+G(d,p) level. Gaussian function is assumed for each peak and half-value widths are changed from $d = 0.05$ to 10.0 G.

Al–NTCDA and $(Al)_3$–NTCDA show hyperfine structures. All spectra become single line spectra if d is assumed to 10.0 G. The peak-to-peak line width ($\Delta H_{pp}$) for 1:1, 1:3 complexes and the dimer are calculated to be 12.0, 6.0 and 5.6 G, respectively.

### 3.5. Simulated IR spectra

Harmonic vibrational frequencies of NTCDA, Al–NTCDA and $Al(NTCDA)_2$ calculated at the B3LYP/6-31G(d) level are illustrated in Fig. 5. In free NTCDA, the frequencies of C=O stretching modes of the carbonyl groups are composed of two peaks appearing around 1830–1863 $cm^{-1}$ (region a). The weak peaks in region b are mainly caused by the C=C stretching mode. The C–O–C stretching and C–C–H bending modes of benzene part are distributed in region c. By the formation of Al–NTCDA complex, the C=O stretching mode is calculated to be 1850 $cm^{-1}$, indicating that the mode is slightly red-shifted by the interaction with the Al atom. The intensity of the C=C stretching mode is largely enhanced in Al–NTCDA, whereas that of the C–O–C mode becomes weaker. In the case of $Al(NTCDA)_2$, a strong peak is appeared at 1374 $cm^{-1}$. This peak is attributed to be a C=O stretching

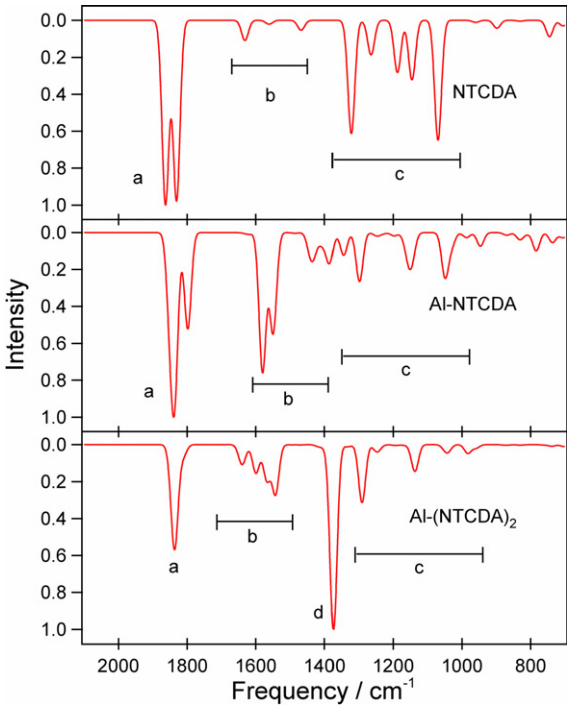


Fig. 5. Harmonic vibrational frequencies of NTCDA, Al–NTCDA, and Al–$(NTCDA)_2$ calculated at the B3LYP/6-31G(d) level.

mode of the C=O carbonyl binding to the Al atom. The values and intensities of vibrational frequencies are in good agreement with the experiment.

### 3.6. Comparison with the experiments

Fig. 6 (upper) shows experimental ESR spectrum of co-deposited film Al–NTCDA. The symmetric line shape with no hyperfine structure is obtained at room temperature. The $g$ value is obtained to be $g = 2.004$, which is slightly larger than that of free electron ($g_e = 2.0023$). Pure NTCDA films are inactive as the ESR spectrum. This result indicates that the co-deposited film Al–NTCDA includes at least a paramagnetic species. The peak-to-peak linewidth ($\Delta H_{pp}$) is measured to be 4.6 G.

The simulated ESR spectra for the 1:1 and 1:3 complexes and bridged dimer are plotted in Fig. 6 (lower), where $d$ is fixed to 10.0 G in all spectra. The bridged dimer and 1:3 complex show reasonable EPR spectra close to the experiment, whereas the EPR spectrum of the 1:1 complex is too wide ($\Delta H_{pp} = 12.0$ G). The peak-to-peak line widths of the metal bridged dimer and 1:3 complex are calculated to be $\Delta H_{pp} = 5.6$ and 6.0 G, respectively. Hence, it seems that the metal bridged dimer and/or 1:3 complex exist in Al/NTCDA co-deposit film.

Fig. 7 shows the experimental absorption spectrum (solid curve) and theoretical values (stick diagram) of the $Al_n$NTCDA and bridged dimer systems. From the comparison with the theoretical calculations, assignment of the absorption spectrum will be possible. The peak $a$ consists of pure NTCDA with $n = 0$. The peaks $b$ and $c$ are contrib-

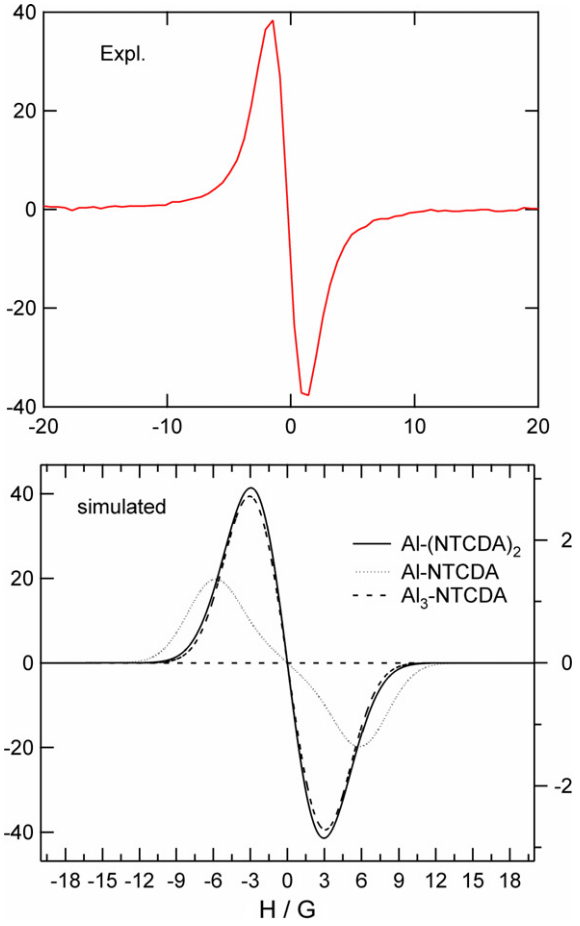


Fig. 6. ESR spectrum of co-deposit film of Al/NTCDA measured at room temperature (upper) and simulated ESR spectra of Al–NTCDA, $Al_3$–NTCDA, and Al–$(NTCDA)_2$ calculated at the B3LYP/6-311+G(d,p) level (lower). Gaussian function is assumed for each peak and half-value width is fixed to $d = 10.0$ G. The experimental spectra is cited from our Ref. [7].

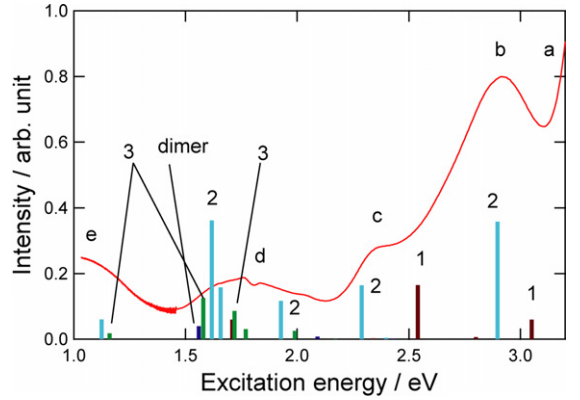


Fig. 7. Experimental and theoretical absorption spectra of Al–NTCDA systems. (Solid curve) experimental spectrum of Al/NTCDA co-deposit film measured at room temperature and (stick diagram) calculated values of $(Al)_n$(NTCDA) ($n = 0$–4) and aluminum metal bridged dimer Al–$(NTCDA)_2$. Number indicates the value of $n$. Intensity of absorption band is in arbitrary unit. The experimental spectrum is cited from our Ref. [7].

uted from both $n = 1$ and 2. The absorption peaks around 1.5–2.0 eV (peak $d$) are composed of $n = 1$–3 and Al-bridged dimer. The peak $e$ is composed of $n = 3$ and bridged dimer. From these theoretical calculations, it is strongly suggested that the experimental absorption spectrum of the Al–NTCDA co-deposited film is not composed of unique species, but the film consists of multi-components such as $Al_n$NTCDA ($n = 0$–4) and the Al-bridged dimer.

## 4. Discussion

In the present study, the metal bridged-NTCDA dimer, the 1:1 and 1:3 complexes have been investigated using DFT method. Main results derived from the calculations are summarized as follows.

(1) The metal bridged-dimer $Al(NTCDA)_2$ has a large binding energy to bind sufficiently two NTCDA molecules. The binding energy calculated at the B3LYP/6-311+G(d) level is 45.5 kcal/mol (22.8 kcal/mol per a Al–O bond).
(2) The binding nature in the 1:1 and 1:3 complexes is consisted of charge-transfer (CT) type where the electron transfer takes place from the metal to NTCDA at the ground state expressed by $(M)_n^{\delta+}(NTCDA)^{\delta-}$ ($n = 1$ and 3). The magnitude of CT ($\delta$) is calculated to be 0.4 at the B3LYP/6-311+G(d,p) level. In the metal bridged-NTCDA dimer, magnitude of CT ($\delta$) is similar to that of the 1:1 complex ($\delta = 0.4$). The electronic state of the bridged NTCDA dimer is schematically expressed by $(NTCDA)^{-\delta/2}M^{+\delta}(NTCDA)^{-\delta/2}$ ($\delta = 0.4$). Namely, the spin densities on NTCDA in the metal bridged-NTCDA dimer becomes half of the 1:1 complex.
(3) The present calculations predicted that ESR spectrum of the metal bridged-NTCDA dimer is much different from that of the 1:1 complex. The peak-to-peak line width in the metal bridged-dimer is significantly narrow than that of Al–NTCDA 1:1 complex and the shape of spectrum is the same as that of the experiment. From comparison of theoretical ESR spectra with the experiments, it is concluded that the Al bridged NTCDA dimer and/or the 1:3 complex are possible to exist in the co-deposit film of Al–NTCDA system.

## Acknowledgements

The authors are indebted to the Computer Center at the Institute for Molecular Science (IMS) for the use of the computing facilities. One of the authors (H.T) also acknowledges a partial support from a Grant-in-Aid for Scientific Research (C) from the Japan Society for the Promotion of Science (JSPS).

## Appendix A. Supplementary material

Supplementary data associated with this article can be found, in the online version, at doi:10.1016/j.jorganchem.2007.08.041.

## References

[1] A. Dodabalapur, Appl. Phys. Lett. 73 (1998) 142.
[2] H. Sirringhaus, N. Tessler, R.H. Friend, Science 280 (1998) 1741.
[3] P.F. Baude, Appl. Phys. Lett. 82 (2003) 3964.
[4] F. Eder, Appl. Phys. Lett. 84 (2004) 2673.
[5] K. Nakayama, M. Umehara, M. Yokoyama, Jpn. J. Appl. Phys. 45 (2006) 974.
[6] K. Nakayama, Y. Niguma, Y. Matsui, M. Yokoyama, J. Appl. Phys. 94 (2003) 3216.
[7] H. Tachikawa, H. Kawabata, R. Miyamoto, K. Nakayama, M. Yokoyama, J. Phys. Chem. B 109 (2005) 3139.
[8] H. Tachikawa, H. Kawabata, J. Mater. Chem. 13 (2003) 1293.
[9] H. Tachikawa, H. Kawabata, Jpn. J. Appl. Phys. 44 (2005) 3769.
[10] H. Tachikawa, H. Kawabata, Phys. Chem. B 107 (2003) 1113.
[11] H. Tachikawa, H. Kawabata, J. Chem. Theor. Comput. 3 (2007) 184.
[12] H. Tachikawa, A. Shimizu, J. Phys. Chem. B 109 (2006) 13255.
[13] Ab initio MO. Frisch, M.J. Trucks, G.W. Schlegel, H.B. Scuseria, G.E. Robb, M.A. Cheeseman, J.R. Zakrzewski, V.G. Montgomery, J.A. Stratmann Jr., R.E. Burant, J.C. Dapprich, S. Millam, J.M. Daniels, A.D. Kudin, K.N. Strain, M.C. Farkas, O. Tomasi, J. Barone, V. Cossi, M. Cammi, R. Mennucci, B. Pomelli, C. Adamo, C. Clifford, S. Ochterski, J. Petersson, G.A. Ayala, P.Y. Cui, Q. Morokuma, K. Malick, D.K. Rabuck, A.D. Raghavachari, K. Foresman, J.B. Cioslowski, J. Ortiz, J.V. Stefanov, B.B. Liu, G. Liashenko, A. Piskorz, P. Komaromi, I. Gomperts, R. Martin, R.L. Fox, D.J. Keith, T. Al-Laham, M.A. Peng, C.Y. Nanayakkara, A. Gonzalez, C. Challacombe, M. Gill, P.M.W. Johnson, B.G. Chen, W. Wong, M.W. Andres, J.L. Head-Gordon, M. Replogle, E.S. Pople, J.A. GAUSSIAN 03, revision A.5; Gaussian, Inc.: Pittsburgh, PA, 2003.